Evidence of noncascade intracenter electron relaxation in shallow donor centers in silicon

S. G. Pavlov,* H.-W. Hübers, and P. M. Haas
Institute of Planetary Research, German Aerospace Center, 12489 Berlin, Germany

J. N. Hovenier and T. O. Klaassen
Kavli Institute of Nanoscience, Delft University of Technology, 2600 GA Delft, The Netherlands

R. Kh. Zhukavin and V. N. Shastin
Institute for Physics of Microstructures, Russian Academy of Sciences, 603950 N. Novgorod, Russia

D. A. Carder and B. Redlich
FOM-Institute for Plasma Physics, 3439 MN Nieuwegein, The Netherlands
(Received 14 July 2008; published 6 October 2008)

Noncascade relaxation of photoexcited electrons on ionized donor centers has been observed in silicon doped by arsenic (Si:As) at low temperatures. Emission spectra of the Si:As terahertz intracenter laser give evidence of specific channels for the electron relaxation through low-lying donor states. The dominating relaxation channels strongly depend on the initial energy distribution of the nonequilibrium carriers. A relaxation step may exceed not only the energy gap to an adjacent lower-lying donor level but also the characteristic energy step as set by the energy and momentum conservation requirements for intravalley acoustic phonons.

DOI: 10.1103/PhysRevB.78.165201 PACS number(s): 72.20.Jv, 71.55.Cn, 78.30.Am, 63.20.kp

I. INTRODUCTION

Relaxation of nonequilibrium charge carriers on ionized and neutral impurity centers in silicon has been thoroughly studied since the 1950s. A major motivation came from the semiconductor electronics applications since electronic capture in silicon determines the speed and efficiency of optoelectronic and electronic devices. In addition, a comprehensive understanding of relaxation processes in doped silicon has become essential for the development of impurity-based silicon lasers and for spin-based quantum information processing.

Originally, a large discrepancy existed between the experimentally measured and theoretically predicted capture rates and cross sections of electrons in silicon. This triggered a long-term theoretical effort to develop an adequate model for the capture of nonequilibrium electrons in silicon for the entire range of temperatures and concentrations as well as for different doping species. The approaches of Lax[1,2] and Ascarelli and Rodriguez,[3] based on a cascade capture model, have brought theoretical values close to the experimentally observed capture rates. The cascade model is based on the assumption that a free carrier is captured not directly into the ground state of an impurity center (which would not explain the large capture rates) but initially into a highly excited state with a large orbit radius. The carriers then relax down the "ladder" of closely spaced energy levels under simultaneous emission/absorption of acoustic phonons.

Lax's model[1,2] neglects the structure and discreteness of impurity states. The energy of an individual relaxation step is determined exclusively by an energy limit $E_{\max}$ on phonons assisting electron relaxation [Fig. 1(a)], which the results form conservation of energy and momentum,[1]

$$E_i^{\max} = (8E_i m_{\text{eff}} v_S^2)^{1/2}, \tag{1}$$

where E_i is the binding energy of the particular donor state, m_{eff} is the electron effective mass, and v_S is the sound velocity in silicon. The typical value of the energy $E_i^{\max}$ is in the range of 0.1–1.5 meV (Fig. 1). The smaller the energy spacing between two states the larger the number of phonons that can assist this relaxation step and, therefore, a higher rate of relaxation between electronic states is expected.

Alternatively, the models of Ascarelli and Rodriguez[3] and Demidov *et al.*[7] account for a dominant relaxation channel through the low angular-momentum hydrogen-type *s* states. Later theoretical approaches[8] made use of the cascade capture model but changed the description by improvement of the semiclassical mathematical apparatus as well as by mak-

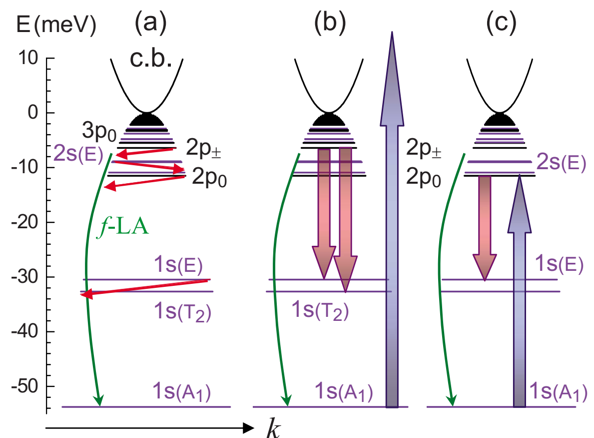

FIG. 1. (Color online) (a) Schematic energy (vs wave vector ***k***) diagram of the impurity levels and electronic relaxation in Si:As. Binding energies for donor levels are taken from Refs. 4–6. The gray color lines indicate even-parity *ns* and *nd* donor levels. Diagonal arrows down show the possible relaxation steps as estimated from the cascade capture model. Curved arrow down indicates the donor-phonon (*f*-LA) resonant relaxation. Bold arrows up are for optical pumping and bold arrows down are for stimulated emission under pumping: (b) far in the CB by emission of a CO_2 laser; (c) in the lowest *p*-type state by the FELIX emission.

 ©2008 The American Physical Society

ing use of the quantized nature of the donor levels. Numerical calculations were also performed.

Because the relaxation step with energies above E_i^{max} cannot be performed with intravalley acoustic phonons, it was assumed[1,9,10] that they are assisted (accompanied) by intervalley phonon or by multiphonon processes. This bottleneck in a capture process may result in relatively long lifetimes of carriers in such excited states.[11,12] The long-living $2p_0$ (we follow the notations of impurity states as in Ref. 4) donor state in Si:P (Ref. 13) and Si:Sb (Ref. 14) has been used to create, through optical pumping, inverted electron populations, leading to intracenter lasing at terahertz frequencies.[15,16] When the difference ΔE between binding energies of particular donor states coincides with the energy of an intervalley phonon in silicon, a resonant electron relaxation takes place from the higher excited state under emission of a phonon. In Si:As, for instance, the resonant nonradiative transition $2s(E) \rightarrow 1s(A_1)$, assisted by the emission of an intervalley longitudinal-acoustic (LA) f phonon [$\Delta E = E_{1s(A_1)} - E_{2s(E)} \approx \hbar\omega_{f\text{-LA}}$; see Fig. 1(a)], has been proposed to determine the intracenter terahertz laser mechanism.[6]

We report here on noncascade relaxation of photoexcited electrons in n-type silicon, deduced from the observed terahertz laser emission spectra of n-Si crystals. From that information as well as from the observed laser thresholds and estimated donor state lifetimes and cross sections for intracenter optical transitions we deduce specific channels of electron relaxation through the low energy donor states. The n-Si spectra have been measured by Fourier transform spectroscopy. The different initial distributions of nonequilibrium carriers in the crystals have been created by selective monochromatic optical excitation of electrons from the $1s(A_1)$ ground state into the donor excited states, starting from the $2p_0$ state and upward into the conduction-band (CB) continuum. Depending on the initial photoexcited state(s), different relaxation schemes have been identified. We observed that a relaxation step in the channels might be larger than the acoustic phonon energy limit E_i^{max}. The probability for nonradiative transitions between impurity states of the same parity and state configurations can exceed that between more closely spaced adjacent states with *unequal* parity and configuration. Intracenter relaxation rates of a number of channels have been estimated using the laser thresholds, as well as data from absorption spectroscopy.

II. EXPERIMENT

Silicon samples used in our experiments had an As concentration of about 3×10^{15} cm^{-3}. They were grown by the float-zone technique along the [100] crystallographic axis. The residual doping (boron) was less than $\sim10^{14}$ cm^{-3}. Final crystals of dimensions $7\times7\times5$ mm^3 had optically polished facets to provide a multimode optical resonator on internal reflections. The experimental setup for observation of terahertz-range lasing from the optically pumped Si:As crystals is shown in Fig. 2. The samples were immersed in a liquid helium (LHe) vessel. Two types of lasers were used as a pump source. A commercial pulsed transversely excited atmospheric (TEA) CO_2 laser (MLT-3 Edinburgh Instruments) tunable over a discrete line spectrum in the wavelength range from 9.2 to 10.6 μm (photon energy of 117–140 meV) was used for photoexcitation of electrons bound to the As ground state [$E_{1s(A_1)}=53.76$ meV (Ref. 4)] into the CB continuum [Fig. 1(b)]. For pumping at energies below the optical phonon [$\hbar\omega_{\text{LTO}}=64$ meV (Ref. 17)], i.e., in the conduction-band bottom and into the discrete As excited states [Fig. 1(c)], the free-electron laser (FEL) FELIX (Rijnhuizen, The Netherlands) was used. The latter source delivers about 5-μs-long macropulses that consist of a train of 5-ps-long micropulses separated by 1 ns time interval and can be tuned over the entire intracenter photoexcitation range needed for Si:As (42–53 meV). In both cases the laser beam passed a variable attenuator before entering a light pipe which guided the radiation to the sample. The [110] sample facet (7×5 mm^2) was irradiated. The terahertz emission was extracted at right angles from the [100] facet (7×7 mm^2). Spectral measurements were performed using a far-infrared Fourier transform spectrometer (FTS) with a spectral resolution of $\sim0.2-0.4$ cm^{-1} equipped with a Ge:Ga photodetector sensitive in the wavelength range from 40 to 120 μm.

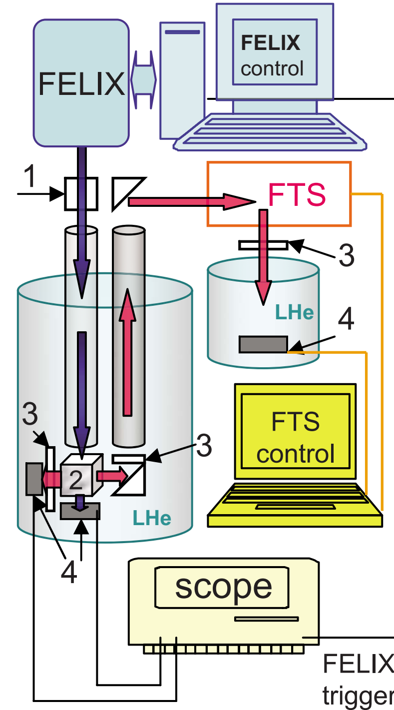

FIG. 2. (Color online) Schematic of experimental setup: (1) FELIX attenuator, (2) Si laser crystal, (3) terahertz filters, and (4) LHe cooled Ge:Ga detectors, FTS is Fourier transform spectrometer.

Stimulated Si:As laser emission is observed when the electrons are excited into the CB state continuum using the TEA CO_2 laser and the FEL at photon energies above the As ionization energy, $\hbar\omega > E_{1s(A_1)}$. For FEL frequencies in the range $\hbar\omega < E_{1s(A_1)}$, laser emission is observed when the pump photon energy coincides with one of the $1s(A_1)\rightarrow np$, nd, nf donor transitions (n is the main quantum number). The laser threshold is found at a pump flux densities above

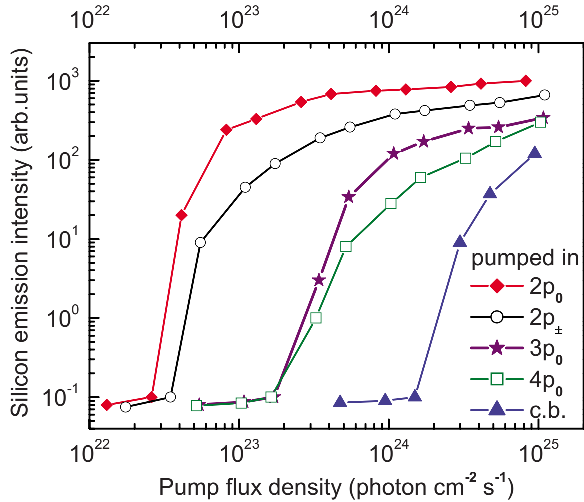

FIG. 3. (Color online) Typical dependences of terahertz silicon laser emission on FELIX pump flux density. The first points corresponding to stimulated emission [i.e., emission order(s) of magnitude above the spontaneous emission, $\sim 10^{-1}$ a.u. on this graph] were taken as the laser threshold value.

$\sim 10^{25}$ photons cm^{-2} s^{-1} for the CO_2 laser and at $\sim 4 \times 10^{22}$ photons cm^{-2} s^{-1} and up for the FEL excitation (photon energy of >42 meV).

Varying the pump frequency results in dramatic changes in the Si:As laser threshold (Fig. 3) and in the emission spectra. Pumping in the $2p_0$ As state [Fig. 4(a)] results in laser emission at 19.90 ± 0.02 meV (160.4 cm^{-1}), which can be attributed to the $2p_0 \rightarrow 1s(E)$ As intracenter transition. This transition exhibits the lowest laser threshold of about 4×10^{22} photons cm^{-2} s^{-1}. The same impurity transition has also been observed in the stimulated emission from the Si:P (Ref. 18) and Si:Sb (Ref. 19) lasers under resonant pumping into the $2p_0$ state. Pumping with photons with an energy coinciding with the next dipole-allowed impurity transition $[1s(A_1) \rightarrow 2p_\pm]$ gives rise to a single emission line originating from the $2p_\pm$ donor state to the $1s(E)$ state [Fig. 4(b)]. The laser threshold for this transition is increased to 6×10^{22} cm^{-2} s^{-1}. Pumping the next allowed transition, $1s(A_1) \rightarrow 3p_0$ [Fig. 4(c)], the $2p_0 \rightarrow 1s(E)$ transition restores the former laser spectrum with the addition of two weaker lines at 24.94 ± 0.02 meV (201.0 cm^{-1}) and 26.33 ± 0.02 meV (212.2 cm^{-1}) that correspond to the arsenic $2p_\pm \rightarrow 1s(E)$ and $2p_\pm \rightarrow 1s(T_2)$ transitions. The lasing originating from the $2p_0$ state disappears again with another step up of the pump photon energy $[1s(A_1) \rightarrow 3d_0]$. Then the transitions originating from the $2p_\pm$ state dominate again [Fig. 4(d)]. These transitions remain when pumping into the $4p_0$ state [Fig. 4(e)]. It must be appreciated that the finite width of the free-electron laser pump radiation [full width at half maximum (FWHM) ≈ 1 meV] results in simultaneous pumping of many states when pumped above $4p_0$ state, so that very closely spaced states with a variety of state configurations and parities are populated, making any analysis meaningless.

Increasing the pump photon energy even further, the $2p_\pm \rightarrow 1s(T_2)$ and $2p_\pm \rightarrow 1s(E)$ transitions persist. Because of a relatively high laser threshold for the $2p_\pm \rightarrow 1s(E)$ emission, this emission is sometimes absent even at the maximum pump power. This is the case, for instance, when pumped by photons with the energy equal to that of the intervalley optical transverse (TO) f phonon [~ 59.1 meV (Ref. 17)]. It should be noted that the Si:As laser emission spectra do not switch wavelength(s) by varying the pump power [from the laser threshold values up to the maximum power available in our experiments (Fig. 3)].

III. DISCUSSION

We discuss now the possible channels of relaxation through the low excited donor states in n-Si based on the spectral measurements for Si:As and other group-V donor Si lasers. Since the np_0, $np_\pm$, nd_0, and $nf_\pm$ states are accurately described by the effective-mass approach,[4] the main differences appear only for the ns states due to the unequal chemical shift of the group-V atoms and the related donor-phonon interactions. The features of the relaxation process deduced here for Si:As can therefore be generalized to the other group-V donor centers in silicon with the exception of the $ns \rightarrow ms$ donor states relaxation due to intervalley phonon resonant interactions.

There are a few clear features seen in the Si:As emission spectra. First of all, the presence of lasing on the $2p_0 \rightarrow 1s(E)$ transition pumped resonantly into the $2p_0$ donor state. This emission has also been observed in Si:P, Si:Sb, and Si:Bi.[18–20] The low lasing threshold for this transition in Si:As clearly indicates that nonradiative relaxation from the $2p_0$ state toward the lower $1s$ states is slow. This results from the absence of appropriate phonon resonances to facilitate the large relaxation steps $2p_0 \rightarrow 1s(E) \rightarrow 1s(A_1)$. Both high energy intravalley and intervalley phonons can contribute to the electron energy relaxation along that path.[9,21]

When pumping at the highest power in the Si:As $2p_\pm$ state, no emission on the $2p_0 \rightarrow 1s(E)$ transition is observed. This proves that nonradiative relaxation from the $2p_\pm$ state is dominated by relaxation into the $2s$ state and not, either directly or via the $2s$ state, into the $2p_0$ state. This finding confirms an assumption made in Ref. 6 about the probable existence of a strong $2s \rightarrow 1s$ relaxation channel that prevents the $2p_0 \rightarrow 1s(E)$ lasing when pumped with a CO_2 laser in the conduction band. Inspecting the energies in question, it can be concluded that the main contribution to this relaxation step arises from interaction of the $2s(E)$ donor state with the f-LA [$\hbar\omega_{f\text{-LA}} \approx 46.3$ meV (Ref. 17)] intervalley phonon. Intravalley transitions between the triplet $ns(T_2)$ and both the singlet $ns(A_1)$ and doublet $ns(E)$ are forbidden due to selection rules.[22] Because the $2s(A_1)$ state [$E_{2s(A_1)} = -10.3$ meV (Ref. 5)] is relatively remote from the resonance with the f-LA phonon, it would suggest that the $2s(E)$ state [$E_{2s(E)} = -8.85$ meV (Ref. 5)] apparently enables this quasiresonant electron relaxation.

We recall here that the same $2s(E) \rightarrow 1s(A_1)$ relaxation shortcut has been found in Si:Bi due to resonant coupling with g-TO intervalley phonons.[23] In Si:Sb the $1s(E) \rightarrow 1s(A_1)$ relaxation shortcut due to resonance with g-TA intervalley phonons was shown to enable intracenter and Raman laser emission.[19] In the case that the $2s - 1s$ transition is

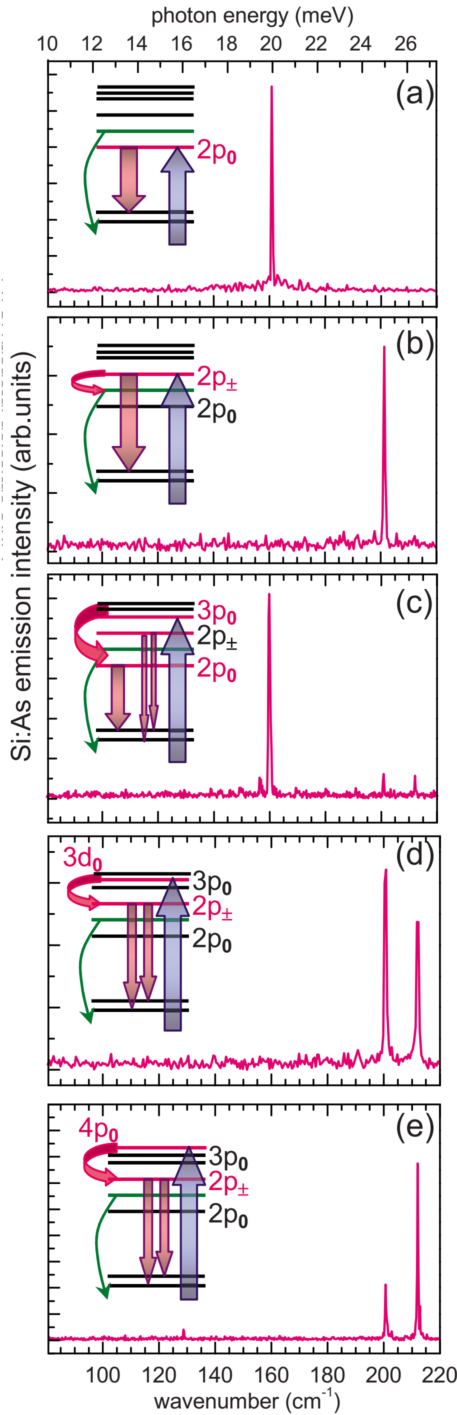

FIG. 4. (Color online) Emission spectra of the Si:As laser under selective intracenter pumping by different FELIX frequencies. Arrows up indicate pumping and arrows down are for the laser emission. Bold curved arrows show the dominant relaxation steps. Insets show the realized laser schemes. The spectra are taken as follows: (a) pump photon energy is 42.47 meV (pumping in the $\rightarrow 2p_0$ state), pump flux density is $\sim 10^{23}$ cm^{-2} s^{-1}; (b) pump photon energy is 47.35 meV ($\rightarrow 2p_\pm$), pump flux density is $\sim 3\times 10^{23}$ cm^{-2} s^{-1}; (c) pump photon energy is 48.28 meV ($\rightarrow 3p_0$), pump flux density is $\sim 2\times 10^{24}$ cm^{-2} s^{-1}; (d) pump photon energy is 49.83 meV ($\rightarrow 3d_0$), pump flux density is $\sim 5\times 10^{24}$ cm^{-2} s^{-1}; and (e) pump photon energy is 50.4 meV ($\rightarrow 4p_0$), pump flux density is $\sim 5\times 10^{23}$ cm^{-2} s^{-1}.

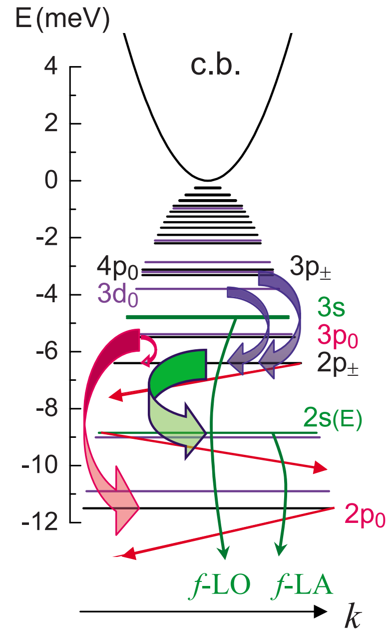

FIG. 5. (Color online) Relaxation channels for low excited states in Si:As. Bold curves indicate the observed dominant relaxation channels with steps by-passing a few adjacent donor states. Width of individual arrows indicates the estimated transition probability. Diagonal arrows down show the size of the of the possible relaxation step as estimated for the cascade capture model. Other arrows are the same as in Fig. 1.

not in resonance with intervalley phonons, such as in Si:P and Si:Sb, a considerable $2s\rightarrow 2p_0$ relaxation takes place, leading to laser emission on the $2p_0\rightarrow 1s(T_2)$ transition when pumped into the $2p_\pm$ state.[16]

The experimental results show that in Si:As the $2p_0$ state can also be populated indirectly by pumping the $3p_0$ state [Figs. 4(c) and 5]. In this case the electrons in the $3p_0$ state relax dominantly into the $2p_0$ state and a relatively small proportion reaches the $2p_\pm$ state. As the $2p_\pm$ state is nearer to the $3p_0$ state, in a cascade relaxation model, the $3p_0 \rightarrow 2p_\pm$ relaxation path would be expected to be the more important.

Pumping into the $3d_0$ donor level, only the $2p_\pm$ state gains an electron population high enough for laser emission. At these relatively high excited donor levels $E^{\max}$ becomes larger than the energy spacing between the adjacent impurity states and intracenter capture should be well described by a classic cascade process. In that case the relaxation of electrons from the $3d_0$ donor state should involve the $3p_0$ state before entering the $2p_\pm$ level. The absence of the $2p_0 \rightarrow 1s(E)$ emission, however, seems to indicate that the $3p_0$ state is by-passed in the relaxation chain or at least its contribution is much less significant than that of the $2p_\pm$ state.

For quantitative estimates of the rates for different relaxation channels of photoexcited electrons we need the values for the cross section of the optical transitions between impurity levels and the lifetimes for the impurity states involved. Although the precise values of the state lifetimes are not known or measured, estimates allow us to show relative relaxation rates as well as their values in the right order of magnitude. We summarize the parameters used for our esti-

TABLE I. Parameters used for estimates of intracenter relaxation rates in Si:As.

Donor state (X)	$2p_0$	$2s$	$2p_\pm$	$3p_0$	$4p_0$
Lifetime τ	38 ± 5 ps	1 ps	30 ± 5 ps	30 ± 5 ps	80 ± 10 ps
Absorption cross sections for optical transitions (terminating donor state X)					
$\sigma_{1s(A_1)\to X}$	$1.7e-14$ cm^2		$5.5e-14$ cm^2	$5.2e-15$ cm^2	$5.0e-15$ cm^2
$\sigma_{1s(E)\to X}$	$9.3e-16$ cm^2		$2.8e-15$ cm^2		
$\sigma s_{1s(T_2)\to X}$	$1.3e-15$ cm^2		$4.2e-15$ cm^2		
Absorption cross sections at laser transition (originating donor state X)					
$\sigma_{X\to 1s(E)}$	$3.0e-15$ cm^2		$2.0e-15$ cm^2		
$\sigma_{X\to 1s(T_2)}$	$4.0e-15$ cm^2		$3.0e-15$ cm^2		

mates in Table I. We limit our consideration to a few lower excited states, where the estimates have relatively low uncertainties.

The cross sections for absorption and emission were taken from a comparative analysis of the known absorption spectra of Si:As at low [T=4–5 K (Refs. 4 and 24)] and elevated [T=60 K (Ref. 25)] temperatures. Additional absorption spectra have been measured for a 1-mm-thick Si:As sample cut from the same material as for the active laser element. This gives the cross section for optical transitions originating from the $1s(A_1)$ ground state, $\sigma_{1s(A_1)\to np}$, in the range of 5×10^{-15}–5×10^{-14} cm^2, and for the emission lines originating from the $2p_0$ and $2p_\pm$ states, $\sigma_{2p_0/2p_\pm\to 1s(E)/1s(T_2)}$, in the range of $(2-4)\times10^{-15}$ cm^2. Absorption due to pumping in the conduction-band continuum is taken to be $\sigma_{1s(A_1)\to \mathrm{CB}}=1.7\times10^{-15}$ cm^2. For estimates of lifetimes τ of the impurity states, the linewidths of the $1s(A_1)\to np$ transitions have been used from the Si:As absorption spectra at 4–5 K (see Table I). The lifetime of the $2s$ state is assumed to be about 1 ps, resulting from its fast decay rate $\tau_{2s}^{-1}\sim10^{12}$ s^{-1} via resonant interaction with the f-LA intervalley phonon.

Next, considering intracenter pumping $[1s(A_1)\to np]$, we will neglect the changes in state populations due to repump transitions into the conduction band ($np\to$CB). For relaxation steps exceeding $E_i^{\max}$ in which nearest-neighbor states are by-passed, we will be interested only in the destination and will not discuss the details of the intermediate levels. We assume that these large steps may occur via a two intervalley phonon "difference" process similar to that described in Ref. 10 for the case of intraband electronic relaxation. We define the population $N_i(J)$ of the state i under the pumping process $j\to i$ with the photon flux density J as

$$N_i(J)=N_j(J)\times J\times\sigma_{j\to i}\times\tau_i.(2).$$

Evidently, at the experimental conditions (T=4 K), the equilibrium population (J=0) of the ground state is $N_{1s(A_1)}(0)\approx N_{\mathrm{As}}$ and all others populations are negligible. The threshold flux density J^{th} will define the threshold population of the impurity state $N_i^{\mathrm{th}}(J^{\mathrm{th}})$ necessary to enable laser action.

Starting from the simplest photoexitation in the $2p_0$ state, we find that even at the highest pump powers in the experiment, there is not sufficient population of the above lying $2p_\pm$ state to cause laser action. This gives an estimate for the maximum rate ν of the relaxation process $2p_0\to2p_\pm$ via the conduction band ($2p_0\to$CB$\to2p_\pm$) as

$$\nu_{2p_0\to2p_\pm}<\tau_{2p_\pm}^{-1}\times N_{2p_\pm}(J_{2p_\pm}^{\mathrm{th}})/N_{2p_0}(J_{2p_0}^{\max})=3\times10^9\ \mathrm{s}^{-1}.$$

This estimate confirms our assumption of the low efficiency (below 10%) of re-excitation from the pumped $2p_0$ state into the CB. The same estimate for the case of pumping in the $2p_\pm$ state shows that the relaxation step $2p_\pm\to2p_0$ has a very low probability $\nu_{2p_\pm\to2p_0}<7\times10^8$ s^{-1}. Since the $2p_\pm$ state decays via the $2s$ and/or $2p_0$ states, its short lifetime, as deduced from absorption spectra, must be due to the dominant channel $2p_\pm\to2s\to1s(A_1)$ with a rate $\nu_{2p_\pm\to2s}>3.3\times10^{10}$ s^{-1}. Pumping in the $3p_0$ state leads to two sets of laser transitions with different thresholds: $J_{3p_0}^{\mathrm{th}2p_0}=3.4\times10^{23}$ photons cm^{-2} s^{-1} for the laser emission at the $2p_0\to1s(E)$ donor transition and $J_{3p_0}^{\mathrm{th}2p\pm}=3.4\times10^{24}$ photons cm^{-2} s^{-1} for the laser emission at the $2p_\pm\to1s(E)$, $1s(T_2)$ donor transitions.

Separating the relaxation channels from the $3p_0$ state, we write its decay as

$$\tau_{3p_0}^{-1}=\nu_{3p_0\to2p_\pm}+\nu_{3p_0\to2p_0}+\nu_{3p_0\to ns}.$$

In this way the probability for the relaxation channel $3p_0\to2p_0$ (energy gap $\Delta E_{3p_0-2p_0}\sim6$ meV$>E_{2p_0}^{\max}$) is estimated to be a factor of 5–6 higher than for the $3p_0\to2p_\pm$ ($\Delta E_{3p_0-2p_\pm}\sim0.9$ meV$\sim E_{2p_\pm}^{\max}$) channel. There remains then a relatively high decay rate due to the other channels, $\nu_{3p_0\to ns}\sim1.4\times10^{10}$ s^{-1}. Probably this rate is so high due to quasiresonances between the donor state pairs $3p_0\leftrightarrow1s(A_1)$ and $3s\leftrightarrow1s(A_1)$ ($\Delta E_{3p_0-1s(A_1)}\sim48.3$ meV, $\Delta E_{3s-1s(A_1)}\sim49.0$ meV) and the f-LO intervalley phonon in silicon (phonon energy of ~48.8 meV).

As already mentioned, the analysis of the results for electrons optically excited into the $3d_0$ state or higher is not very meaningful. It is clear however that the $2p_\pm$ state plays an important role in the relaxation channels in that case.

We will summarize below the identified high-probability relaxation channels or intracenter relaxation for the low excited states of shallow donors in silicon (Fig. 5):

$$1s(E) \rightarrow 1s(A_1),$$

in case of resonance with intervalley phonon (Si:Sb, Si:P) as deduced from the experiments[16,19] and calculated in Ref. 21: $\nu_{1s(E)\rightarrow 1s(A_1)} > 10^{11}\ \mathrm{s}^{-1}$,

$$2s(E) \rightarrow 1s(A_1),$$

in case of resonance with intervalley phonon [Si:As, Si:Bi (Refs. 6 and 19)],

$$3p_0 \rightarrow 2p_0, \quad \nu_{3p_0\rightarrow 2p_0} \sim 1.3 \times 10^{10}\ \mathrm{s}^{-1},$$

$$2p_\pm \rightarrow 2s(E), \quad \nu_{2p_\pm\rightarrow 2s} > 3.3 \times 10^{10}\ \mathrm{s}^{-1},$$

$$3d_0 \rightarrow 2p_\pm \rightarrow 2s(E),$$

$$3p_\pm, 4p_0 \rightarrow 2p_\pm \rightarrow 2s(E), \quad \nu_{4p_0\rightarrow 2p_\pm} > 1.5 \times 10^{10}\ \mathrm{s}^{-1}.$$

As can be seen in Fig. 3, the lasing threshold for pumping near to the conduction-band edge is much larger than for pumping lower excited states. That is mainly due to the many possible relaxation channels that causes the initial electron population to spread widely.

Because of this multichannel broadening, a significant part of the excited electrons evidently does not reach the relatively long-living $2p_0$ and $2p_\pm$ donor states, instead using the alternative $3s \rightarrow 2s \rightarrow 1s$ channel where possible. This effect causes the low efficiency of the terahertz silicon laser pumped by a CO_2 laser.

IV. SUMMARY

In summary, we have shown that nonequilibrium electrons in moderately doped silicon at low temperatures relax via low donor states by selected channels that depend on the initial state. A relaxation step in the channels can exceed the energy limit that follows from momentum and energy conservation for acoustic phonons. The relaxation rate between impurity states of the same parity and state configurations can exceed the one between more closely lying neighboring levels. Significant influence on the relaxation rates in silicon can be obtained by applying an external deformation to a crystal[26] that modifies the electron-phonon interaction.

ACKNOWLEDGMENTS

This work was partly supported by the Investitionsbank Berlin, the Deutsche Forschungsgemeinschaft, and the Russian Foundation for Basic Research (Grants No. 436 RUS 113/937/0-1, No. 08-02-91951, and No. 08-02-00333). We gratefully acknowledge the support by the Stichting voor Fundamenteel Onderzoek der Materie (FOM) in providing the required beamtime on FELIX and highly appreciate the skilful assistance by the FELIX staff.

*Corresponding author. Institute of Planetary Research, German Aerospace Center, Rutherfordstrasse 2, D-12489 Berlin, Germany. FAX: +49 (0)30 67055507. sergeij.pavlov@dlr.de

[1] M. Lax, J. Phys. Chem. Solids **8**, 66 (1959).

[2] M. Lax, Phys. Rev. **119**, 1502 (1960).

[3] G. Ascarelli and S. Rodriguez, Phys. Rev. **124**, 1321 (1961); **127**, 167 (1962).

[4] A. K. Ramdas and S. Rodriguez, Rep. Prog. Phys. **44**, 1297 (1981).

[5] Theoretically calculated values for *s*-type states are taken from Y. C. Chang, T. C. McGill, and D. L. Smith, Phys. Rev. B **23**, 4169 (1981).

[6] H.-W. Hübers, S. G. Pavlov, R. Kh. Zhukavin, H. Riemann, N. V. Abrosimov, and V. N. Shastin, Appl. Phys. Lett. **84**, 3600 (2004).

[7] E. V. Demidov, M. C. Kuznetsov, V. V. Tsyplenkov, and V. N. Shastin, Proceedings of the Workshop "Nanophysics", N. Novgorod, Russia, 13–17 March 2006 (unpublished), Vol. 2, p. 320.

[8] D. R. Hamann and A. L. McWhorter, Phys. Rev. **134**, A250 (1964); E. F. Smith and P. T. Landsberg, J. Phys. Chem. Solids **27**, 1727 (1966); A. Palma, J. A. Jiménez-Tejada, A. Godoy, J. A. López-Villanueva, and J. E. Carceller, Phys. Rev. B **51**, 14147 (1995).

[9] T. G. Castner, Phys. Rev. **130**, 58 (1963).

[10] Y. B. Levinson, Solid-State Electron. **21**, 923 (1978).

[11] A. Lehto and W. G. Proctor, J. Phys. C **11**, 2239 (1978).

[12] Ya. E. Pokrovskii, O. I. Smirnova, and A. Khvalkovskii, J. Exp. Theor. Phys. **85**, 121 (1997).

[13] S. G. Pavlov, R. Kh. Zhukavin, E. E. Orlova, V. N. Shastin, A. V. Kirsanov, H.-W. Hübers, K. Auen, and H. Riemann, Phys. Rev. Lett. **84**, 5220 (2000).

[14] S. G. Pavlov, H.-W. Hübers, H. Riemann, R. Kh. Zhukavin, E. E. Orlova, and V. N. Shastin, J. Appl. Phys. **92**, 5632 (2002).

[15] H.-W. Hübers, S. G. Pavlov, M. Greiner-Bär, M. F. Kimmitt, M. H. Rümmeli, R. Kh. Zhukavin, H. Riemann, and V. N. Shastin, Phys. Status Solidi B **233**, 191 (2002).

[16] H.-W. Hübers, S. G. Pavlov, and V. N. Shastin, Semicond. Sci. Technol. **20**, S211 (2005).

[17] M. Asche and O. G. Sarbei, Phys. Status Solidi B **103**, 11 (1981), and references therein.

[18] R. Kh. Zhukavin, D. M. Gaponova, A. V. Muravjov, E. E. Orlova, V. N. Shastin, S. G. Pavlov, H.-W. Hübers, J. N. Hovenier, T. O. Klaassen, H. Riemann, and A. F. G. van der Meer, Appl. Phys. B: Lasers Opt. **76**, 613 (2003).

[19] S. G. Pavlov, H.-W. Hübers, J. N. Hovenier, T. O. Klaassen, D. A. Carder, P. J. Phillips, B. Redlich, H. Riemann, R. Kh. Zhukavin, and V. N. Shastin, Phys. Rev. Lett. **96**, 037404 (2006).

[20] V. N. Shastin, R. Kh. Zhukavin, E. E. Orlova, S. G. Pavlov, M. H. Rümmeli, H.-W. Hübers, J. N. Hovenier, T. O. Klaassen, H. Riemann, I. V. Bradley, and A. F. G. van der Meer, Appl. Phys. Lett. **80**, 3512 (2002).

[21] E. E. Orlova, Electronic Proceedings of the 26th International Conference Physics of Semiconductor, Edinburgh, UK, 2002 (unpublished), p. 61.

[22] A. Griffin and P. Carruthers, Phys. Rev. **131**, 1976 (1963).
[23] N. R. Butler, P. Fisher, and A. K. Ramdas, Phys. Rev. B **12**, 3200 (1975).
[24] C. Jagannath, Z. W. Grabowski, and A. K. Ramdas, Phys. Rev. B **23**, 2082 (1981).
[25] A. J. Mayur, M. D. Sciacca, A. K. Ramdas, and S. Rodriguez, Phys. Rev. B **48**, 10893 (1993).
[26] S. G. Pavlov, U. Böttger, H.-W. Hübers, R. Kh. Zhukavin, K. A. Kovalevsky, V. V. Tsyplenkov, V. N. Shastin, N. V. Abrosimov, and H. Riemann, Appl. Phys. Lett. **90**, 141109 (2007).